Electron-emission yield of Al, Cu, and Au for the impact of swift bare light ions

O. Benka, A. Schinner, T. Fink, and M. Pfaffenlehner
Institut für Experimentalphysik, Johannes Kepler Universität, Alternbergerstrasse 69, A-4040 Linz, Austria
(Received 21 April 1995; revised manuscript received 22 June 1995)

The electron emission yield induced by mega-electron-volt H^+, He^{2+}, Li^{3+}, B^{5+}, and C^{6+} impact on aluminum, copper, and gold targets was measured. We found a significant deviation of the results from a simple proportionality to the stopping power, especially for heavier ions and low projectile velocities. Using a slightly modified model by J. E. Borovsky and D. M. Suszcynsky [Phys. Rev. A **43**, 1433 (1991)] our experiments could be well represented. In this model the collective electric field generated along the projectile's path was taken into account. Consequently, the positive ion channel appears to be the dominant mechanism that leads beyond a projectile-independent yield–to–stopping power ratio.

PACS number(s): 34.50.Dy, 79.20.Nc

I. INTRODUCTION

The interaction of swift charged particles with solid surfaces leads to ion-induced electron emission (IIEE). Kinetic electron emission is the most important process for ion velocities $v > 10^8$ cm/s. Various aspects of this kinetic IIEE process have been studied for a long time. A survey of these investigations is given in recent reviews by Hasselkamp [1] and Rothard, Groeneveld, and Kemmler [2]. One of the important quantities to describe IIEE is the mean number of emitted electrons per incident ion, the electron emission yield γ. According to the most common theoretical models [3,4] γ is related to the energy deposited by the impinging ion in the surface layer with a thickness, which is equal to the mean escape depth of the emitted electrons. For fast light ion impact, where nuclear energy loss can be neglected, γ should be proportional to the stopping power $S = -dE/dx$ of the target to the ion of energy E:

$$\gamma = \Lambda S, \tag{1}$$

with Λ depending only on the target material, not on the impinging ion.

This basic relation (1) was studied in several investigations (Refs. [1,2] and references therein). Since γ depends critically on surface conditions, ultrahigh vacuum and careful target preparation are necessary to obtain reliable results. Nevertheless, there are only few experimental data available which have been measured under the above requirements.

For C targets and a large amount of different ions Λ is found to be roughly a constant with systematic deviations of 30% [5]. For metal targets and H^+ projectiles Λ is measured for a wide range of velocities and is also found to be constant [1]. This fact is also corroborated by a Monte Carlo simulation for aluminum targets [6]. For projectiles with atomic numbers $Z > 1$ it is always found that Λ decreases with increasing Z [2]. Some authors claim that Λ depends on Z only, and not on the ion velocity for fast ions. Clouvas *et al.* [7] proposed a scaling law $\Lambda(Z) = \Lambda(1)Z^{-0.2}$ for C foils. Borovsky and Suszcynsky [8] also experimentally find Z^a scaling for Λ, where a depends on the target material.

On the other hand, it was found recently [9] that for Ag and Au targets, and He^{2+} impact Λ depends on the ion velocity. Koyama *et al.* [10] also found for metal targets and high energetic bare ions a velocity dependence of Λ.

Different models are proposed to explain the experimental results. Rothard *et al.* [5,11] claim that the reduction of electron yield is mainly due to preequilibrium stopping power, which is different from the equilibrium stopping power used for evaluating Λ. They point out that using an appropriate stopping power S_{eff}, which takes the charge state of the projectile in the surface layer into account, Λ does not depend on the projectile.

Borovsky and Suszcynsky [8] used for projectiles swift bare ions with no bound electrons, where charge changing processes in the surface region can be excluded, and where the stopping power can be reasonably well calculated. Their experimental results can therefore not be explained by preequilibrium effects of stopping power. They propose a reduction of electron yield by collective electric fields within the metal. According to their model the reduction and therefore also the change of Λ does not depend only on Z, but also on the ion velocities. In their experiments they used only very fast ions (1.5–11 MeV/u), where this velocity dependence is not observed.

The aim of this paper is to investigate in more detail the dependence of the IIEE yield γ on projectile properties and to clarify the question of the velocity dependence of Λ. Only bare ions are used in order to have well-defined projectiles (no stripped electrons) in the surface region of the targets, with no charge changing processes. The experimental results are compared to the slightly modified model of Borovsky and Suszcynsky [12], and very good agreement is found. Fitting parameters of this model to our data target material constants are obtained, which can now be used in place of Λ to calculate the IIEE yield γ for different ions.

II. EXPERIMENT

The IIEE yield γ of Al, Cu, and Au targets was measured for impinging H^+, He^{2+}, Li^{3+}, B^{5+}, and C^{6+} ions. The energy of the ions was between 0.5 MeV (H^+) and 8 MeV. Measurements were performed by the charge integration method and by the emission statistic method. The experimental setups are described in detail in Refs. [9] and [13].

The projectiles were obtained from the 1.6-MV tandem

accelerator of Linz University. After energy selection the projectiles could be stripped of their electrons by passing through a thin carbon foil. The ions were then charge state analyzed in a switching magnet before entering the beam line, which leads to the UHV measuring chamber. The beam line vacuum system (10^{-6} mbar) was separated from the UHV chamber by a differentially pumped beam entrance chamber (10^{-8} mbar). In the UHV chamber a working pressure of 3×10^{-10} mbar was obtained with all valves open to the beam line.

The targets were produced by evaporation on stainless steel or silicon backings. After preparation the targets were moved to a manipulator in the UHV chamber without breaking the vacuum. The thickness of the evaporated layers was 100–400 $\mu g/cm^2$, which is much larger than the mean escape depth of the electrons. Before beginning the yield measurements all targets were sputter cleaned using 2-keV Ar ions until no carbon contamination was visible in an Auger electron spectrometer. At the working pressure of 3×10^{-10} mbar the surfaces remained clean for several hours, and the measured yields were reproducible within 1%. Within 1 d we got for Al and Au targets an increase of the yield of about 3% due to contamination. For Cu a decrease of about 2% was found in contrast to the often stated assumption that clean metal surfaces have the lowest IIEE yield and contamination increases the yield [1,5].

The setups for measurement of γ via charge integration (CI) and via emission statistics (ES) were each mounted on flanges, which could easily be changed. In the CI setup the target was at ground potential and the Faraday cup at a potential of 170 V in order to collect electrons emitted from the target. The currents from the target and the Faraday cup were measured by picoammeters and integrated to give the corresponding charges.

For measurements by the ES method the target was at a potential of -20 kV so that the emitted electrons were accelerated and focused to a solid state vector (passivated implanted planar silicon type). From the measured electron energy spectra emission amplitudes C_n were evaluated, which gave the number of events for emission of $n=1,2,\ldots,$ electrons. In the evaluation procedure, which is described in detail in Ref. [13], backscattering of the electrons in the detector is taken into account. All measured distributions of C_n could be fitted very well to a Pólya distribution [13].

The emission yield γ was obtained from

$$w_n = C_n \left(\sum_{n=0}^{\infty} C_n \right)^{-1} \tag{2}$$

and

$$\gamma = \sum_{n=1}^{\infty} n w_n . \tag{3}$$

The amplitude C_0 cannot be measured directly by ES. In the evaluation C_0 was extrapolated from the fitted Pólya distribution. For $\gamma>4$, C_0 is very small and the error of this extrapolation becomes negligible. Consequently, we only used γ values of ES measurements for $\gamma>4$. The smaller γ values were taken from the CI measurements.

TABLE I. Experimental emission yields γ for perpendicular impact of bare ions on Al, Cu, and Au.

	Energy	Targets		
Projectile	(MeV)	Al	Cu	Au
H^+	0.5	0.774	1.35	1.68
	1.0	0.535	.97	1.27
	2.0	0.349	0.651	0.91
	3.0	0.267	0.503	0.72
He^{2+}	1.2	3.40	5.22	6.03
	2.0	2.81	4.68	5.60
	3.0	2.29	4.01	4.91
	4.0	1.98	3.55	4.45
	4.8	1.80	3.23	4.20
Li^{3+}	0.8	6.57	7.70	8.40
	2.0	6.16	8.55	9.91
	3.2	5.51	8.38	10.14
	4.8	4.78	7.69	9.50
	6.4	4.24	7.07	8.91
B^{5+}	2.0		14.6	16.9
	3.2	11.7	15.5	18.1
	4.8	11.1	15.6	18.8
	6.4	10.7	15.2	18.6
	8.0	10.2	14.8	18.3
C^{6+}	3.2	14.3	19.2	20.7
	4.8	13.8	19.6	22.5
	6.4	13.3	19.1	22.7
	8.0	12.9	18.7	22.8

For several target-projectile combinations γ was measured by both methods and agreement was found within 2%. The ES values were always slightly higher for about 1.5%. The reproducibility of both methods was about 1%. As a final result a mean value of measurements by both methods was taken. If γ was measured by one method only, the result was corrected by $+1\%$ for CI and -1% for ES. The final uncertainties of the γ values are estimated to be about 2–3%. For Li^{3+} and C^{6+} ions only the high-energy points could be measured by the CI method, because for this method a much larger ion current is necessary than for the ES method. The B^{5+} γ values were only measured by ES. Numerical results of the obtained γ values are given in Table I.

III. STOPPING POWER OF BARE IONS

For comparison of the experimental IIEE yields with the predictions of Eq. (1) or the model of Borovsky and Suszcynsky the knowledge of the stopping power for bare ions is necessary. Because all published tabulated stopping power values are for ions in charge equilibrium, these values cannot be used, except those for H^+. Only very few data are published for bare ions with $Z>1$ [14,15], but the energy range investigated there is much higher than the energies of the ions used in the present work. Consequently, an estimation of

stopping power values had to be made.

We follow the successful approach by Ziegler, Biersack, and Littmark [16], who start from the stopping power $S_H(v)$ of a proton with velocity v to calculate the stopping power of a heavier ion in charge equilibrium. An effective charge Z_{eff} (which is close to the equilibrium charge of swift ions in condensed matter [16,17]) is introduced there, in order to estimate the stopping power for this ion by $Z_{eff}^2 S_H(v)$. In the case of *bare* ions ($Z_{eff}=Z$) this leads to the straightforward estimation of their stopping power $S_Z(v)$

$$S_Z(v)=Z^2 S_H(v). \tag{4}$$

Here and in the following we designate $S_H(v)$, i.e., the proton stopping power, to be an input quantity to our theoretical analysis. Later on we shall obtain it from a fit of experimental data [16], but it could as well be taken from other sources, e.g., a sophisticated theory.

Now, in order to check the validity of the estimation, Eq. (4), we compare it with a state of the art theoretical calculation for bare ions: recently, Andersen *et al.* [18] have given a survey of the energy loss of heavy ions at high velocities. Following Ref. [18] the theoretical stopping power S_{th} can be written as

$$S_{th}=\frac{4\pi e^4 n Z_t}{mv^2} Z^2 L, \tag{5}$$

where n is the density of target atoms, Z_t is the atomic number of the target, v is the velocity of the projectile, m and e are the mass and charge of the electron, and L is the stopping number. It is composed of the Bethe term L^{Be} with the Barkas and Bloch corrections B and ΔL^{Bl}:

$$L=(L^{Be}-\Delta L^{Bl})(1+B). \tag{6}$$

The Bethe term is given by

$$L^{Be}=\ln\left(\frac{2mv^2}{I}\right)-C_S, \tag{7}$$

where I is the mean ionization potential, and C_S is the so-called shell correction. We now took the shell correction into account by introducing a corrected mean ionization potential I_{corr}, defined via

$$S_H=\frac{4\pi e^4 n Z_t}{mv^2}\left[\ln\left(\frac{2mv^2}{I_{corr}}\right)-\Delta L^{Bl}\right](1+B), \tag{8}$$

and setting

$$L^{Be}=\ln\left(\frac{2mv^2}{I_{corr}}\right). \tag{9}$$

The Bloch correction is given by

$$\Delta L^{Bl}\cong\left(\frac{\kappa}{2}\right)^2\sum_{n=1}^{100}\frac{1}{n[n^2+(\kappa/2)^2]}, \tag{10}$$

with $\kappa=2Zv_0/v$, and v_0 being the Bohr velocity. The Barkas correction B was set as

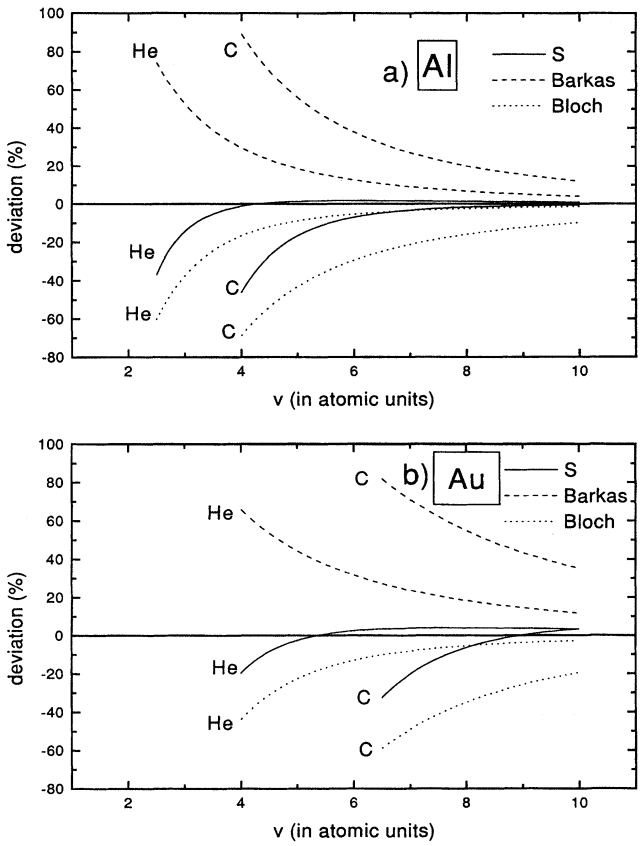

FIG. 1. Contributions and deviations, respectively, of the stopping power vs projectile velocities for impact of He and C ions on (a) aluminum and (b) gold. Contributions of the Barkas term (dashed line) and of the Bloch term (dotted line) to the stopping power S [Eq. (5)], and deviation of the stopping power S from S_Z [Eq. (4)] (full line) are shown.

$$B+\frac{2Z}{\sqrt{Z_t}}F\left(\frac{v}{v_0\sqrt{Z_t}}\right). \tag{11}$$

The function F, which is defined in [19], was approximated by

$$F(x)=0.33x^{-(2+0.17\ln x)}. \tag{12}$$

The full lines in Fig. 1 show the percentile deviations of the stopping power estimations S_Z (using experimental values for S_H [16]) and S_{th}, for He^{2+} and C^{6+} on Al and Au targets. Furthermore, the individual contributions of the Barkas and Bloch corrections to S_{th} are shown. It can be seen that the corrections have different signs and almost cancel each other. S_{th} does not deviate more than 10% from S_Z for Barkas and Bloch corrections smaller than 50%. Corrections larger than 50% are considered to be unreliable.

Since within its range the applicability S_{th} is close to S_Z, we finally use the simple S_Z values as stopping power for bare ions in our further calculations. Besides the greater simplicity this also has the advantage that it can be used for values of small projectile velocities, where S_{th} already breaks down.

IV. THEORETICAL ANALYSIS

A. The Borovsky-Suszcynsky model

In this subsection we give a brief summary of the model by Borovsky and Suszcynsky [12] for the total emission yield. This is intended as a convenience for the reader, who should refer to Ref. [12] for greater detail.

In the phenomenological model of Sternglass [3], the total yield of emitted secondary electrons γ_0 (the subscript "0" denotes the uncorrected value) is assumed to be linearly proportional to the projectile stopping power S [cf. Eq. (1)]

$$\gamma_0 = \frac{P d_s}{E_*} S. \tag{13}$$

The prefactor $P d_s / E_*$ typically is of order 0.1 Å/eV, and is composed of the mean escape depth d_s, and the escape probability P for the emitted electrons, divided by the average amount of energy E_* necessary for a single ionization process.

To go beyond this simple picture Borovsky and Suszcynsky have suggested modifications of the Sternglass ansatz that account for wake field effects and dynamic sheathe within the metal target: the impinging ion is creating a cylindrical positive channel of radius r_{ch} along its path through the target, which is the source for an electric trap potential $\Delta\Phi_{\mathrm{trap}}$, making it more difficult for the outmoving swarm of excited electrons to escape. The ion channel itself has a finite lifetime due to dynamic shielding by the electron collective. Thus one obtains for the corrected total emission yield γ

$$\gamma = \gamma_0 \left[\frac{1}{I} - \frac{1}{2mv^2} \right]^{-1} \left[\frac{1}{I + e\Delta\Phi_{\mathrm{trap}}} - \frac{1}{2mv^2} \right], \tag{14a}$$

$$e\Delta\Phi_{\mathrm{trap}} = \frac{e^2 F_{\mathrm{casc}} \gamma}{P d_s} \left[1 + 2 \ln\left(\frac{r_{\max}}{r_{\mathrm{ch}}} \right) \right], \tag{14b}$$

$$r_{\max} = \frac{5\tau_P}{6\pi} \left[\frac{2e^2 F_{\mathrm{casc}} \gamma}{P d_s m} \right]^{1/2}, \tag{14c}$$

$$r_{\mathrm{ch}} = 2Ze^2 \left\{ \frac{1}{2mv^2} \left[\frac{1}{\Delta E_{\mathrm{ch}}} - \frac{1}{2mv^2} \right] \right\}^{1/2}. \tag{14d}$$

Therein I denotes the mean ionization energy of the target material. $2mv^2 \equiv E_{\max}$ is the maximal energy transferred from the projectile to an electron in a single collision, with m and v being the electron mass and projectile velocity, respectively. F_{casc} is defined as the fraction of the secondary electrons that are directly produced by the projectile, not by cascade processes. Z denotes the projectile's (effective) charge state, while ΔE_{ch} is the energy kick that defines the ion channel radius r_{ch}. Finally, $r_{\max}$ is the classical turnaround radius for an electron moving in the trap potential with such initial velocity that it reaches $r_{\max}$ exactly at the time $\tau_P/3$, when the wake field is "turned off" by the screening conduction band electrons; τ_P is the plasma period of the metal target. The stopping power S enters the model via γ_0 and Eq. (14a), and is to be treated, on principle, as an experimental input quantity. As already discussed in the previous section, we actually used measured values for proton impact, combined with a Z^2 scaling law of the projectile charge state Z.

Within this model the secondary electrons moving away from the ion channel created by the impinging projectile are losing energy by climbing out of the trap potential well. This energy is transferred into the nondirectional motion of the screening cloud, which totally shields the positive background charge after a time $\tau_P/3$, and consequently the energy is no longer available for the excitation or escape of secondary electrons. Thus, this physical mechanism always reduces the total emission yield γ with respect to the uncorrected value γ_0.

B. Modifications of the model

For small projectile velocities the maximal energy transfer $E_{\max} = 2mv^2$ can approach or even be smaller than the mean ionization energy I. In this case the model obviously breaks down, as is seen directly from Eq. (14a). Especially for gold targets and heavy projectiles the range of validity of the present model is dramatically reduced, which makes it impossible to satisfactorily compare the theory with our experiments. The usual concept of the mean ionization energy, however, is principally restricted to the situation where the impinging projectile can distribute a maximal energy kick much larger than I. As $E_{\max}$ decreases, other excitation channels with smaller energies, down to the Fermi energy of the electron gas, are growing in importance. To overcome this obstacle, one should bear in mind that the assumptions leading to Eq. (14) are on the same theoretical level as those leading to the well-known Bethe formula [Eq. (5) with $L = L^{\mathrm{Be}}$] for the electronic stopping power. Consequently, the Bethe theory also breaks down in the same range of projectile velocities. Thus, as a straightforward solution for the breakdown of Eq. (14) we introduce an effective mean ionization potential I^{eff}, which is defined via the equation

$$S_{\mathrm{H}} = \frac{4\pi n Z_t e^4}{mv^2} \ln\left(\frac{2mv^2}{I^{\mathrm{eff}}} \right), \tag{15}$$

where S_{H} has been introduced via Eq. (4); n and Z_t denote the target lattice density and atomic number, respectively. One has to bear in mind clearly that this effective ionization potential conceptionally differs from that one introduced in

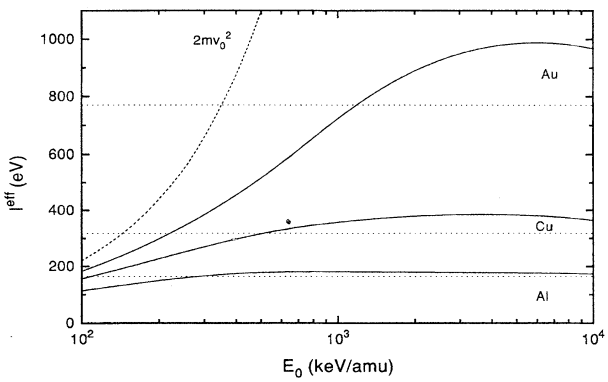

FIG. 2. Effective mean ionization potential I^{eff} of Al, Cu, and Au [Eq. (15)] vs projectile energy/mass E_0 (full lines). Dotted lines: mean ionization potential I [21]. Dashed line: maximum energy transferred to an electron.

Sec. III via Eq. (8). The actual values of I^{eff} as a function of the projectile velocity for aluminum, copper, and gold targets can be seen in Fig. 2. Using I^{eff} rather than I in Eq. (14) leads to significantly improved results.

In the original work by Borovsky and Suszcynsky the parameter ΔE_{ch} was set to $I/2$. Since the ion channel width should be defined by the average (effective) ionization energy needed to free an electron, we are using $\Delta E_{\text{ch}} = I^{\text{eff}}$ instead. The actual choice of ΔE_{ch}, however, does not significantly influence the results, since this quantity enters the theory as argument of a logarithm [cf. Eq. (14b)].

C. High-velocity approximation

In Fig. 7 of the original work by Borovsky and Suszcynsky [12] it is seen that, at least in the energy range considered there, the results of their model for various projectiles almost lie on a single curve, independent of the projectiles' atomic numbers, if one plots γ/γ_0 versus γ_0. As already mentioned by Borovsky and Suszcynsky, this is only true in the limit of very high projectile energies, whereas for lower velocities, the "universal" curve clearly splits into a group of curves, individual for each projectile charge. Nevertheless, it is interesting to take a closer look at the high-energy limit of this model, since there the coupled equations (14) can be reduced to a closed formula.

Under the assumption that the projectile energy $E \gg I$, one can replace Eq. (14a) by

$$\gamma \cong \gamma_0 \frac{I}{I + e\Delta\Phi_{\text{trap}}}. \tag{16}$$

Furthermore, the actual solution will differ only by a small amount from the free yield γ_0, so that the appearance of γ in $r_{\max}$ can be approximated by γ_0. The combination of Eqs. (14a) and (14b) then leads to a simple quadratic equation with the solution

$$\gamma = \frac{1}{A}(\sqrt{1+2A\gamma_0} - 1), \tag{17}$$

with

$$A = \frac{4a_B \mathscr{R}}{Pd_s I} F_{\text{casc}}(1 + \ln R) \tag{18a}$$

and

$$R = \frac{25}{9} F_{\text{casc}} \frac{\Delta E_{\text{ch}} a_B}{(\hbar\omega_P)^2 E_*} m v^2 S_{\text{H}}(v), \tag{18b}$$

where $\mathscr{R} = \nearrow$ Ry. Again, S_{H} denotes the proton stopping power, a_B stands for the Bohr radius, and ω_P is the plasma frequency. Unfortunately, the quantity R still explicitly contains the projectile velocity. Approximating the proton stopping power by the Bethe formula [i.e., Eq. (15) with $I^{\text{eff}} = I$], and neglecting the logarithmic dependence on $E_{\max}$ (since R itself is the argument of a logarithm), one finally obtains

$$R \approx \frac{400\pi}{9} F_{\text{casc}} \left(\frac{\mathscr{R}}{\hbar\omega_P}\right)^2 \frac{\Delta E_{\text{ch}}}{E_*} Z_t n a_B^3 \ln\left(\frac{2mv_c^2}{I}\right). \tag{19}$$

TABLE II. Results of fitted parameters of Eqs. (14) and (17) for Al, Cu, and Au targets.

Target	Λ (Å/eV)	Pd_s (Å)	F_{casc}	A
Al	0.120	3.3	0.45	0.138
Cu	0.094	3.7	0.39	0.073
Au	0.103	3.1	0.28	0.031

Therein the quantity v_c is a characteristic constant high projectile velocity, which does not sensitively enter the quantitative results. We have set it to $v_c = 10v_0$, corresponding to a projectile velocity of approximately $\frac{1}{10}$ of the light speed, a limit, beyond which relativistic effects are becoming important, anyway. Thus the parameter A in Eq. (17) is now a function of target properties only.

V. RESULTS AND DISCUSSION

Applying this model to our experiments, one has to dispose of the three remaining unknown target-depending parameters, Pd_s, F_{casc}, and E_*. First we used the abbreviation $\Lambda \equiv Pd_s/E_*$, introduced in Eq. (1), to replace the parameter E_*, since Λ is more directly accessible to measurements than is E_*. We then fitted Eq. (14), in a least mean square sense to our experimental results. As already mentioned in Sec. II the projectile stopping power S [for evaluation of Eq. (13)] was calculated using S_Z of Eq. (4); the S_{H} values were taken from the work by Ziegler, Biersack, and Littmark [16]. The resulting optimal values for the three fit parameters are listed in Table II.

It is especially noteworthy that the cascade factor F_{casc} is closely related to the statistics of particle-induced electron emission, as we have investigated in a previous paper [20]: the probability of producing n electrons with a single projectile is given by a Pólya distribution

$$P_n(\mu, b) = \frac{\mu^n}{n!}(1 + b\mu)^{-n-1/b} \prod_{i=1}^{n} [1 + (i-1)b] \tag{20}$$

with mean value $\mu = \gamma$ and parameter b. Within a semiempirical model we have shown that the parameter b has the physical meaning of a cascade strength, and can be quantitatively estimated in excellent agreement with the experiment. Following the approach outlined there, the connection between F_{casc} and b is given by

$$F_{\text{casc}} \approx \frac{1}{1 + b\gamma}. \tag{21}$$

Within first approximation F_{casc} should be independent of the type of ion and its velocity. In Eq. (21) both b and γ depend on the properties of the projectile, but the dependencies coarsely cancel each other. Mean values of F_{casc} are 0.43 for Al, 0.5 for Cu, and 0.44 for Au, obtained from emission statistics measurements [20] of the Pólya parameter b for 1-, 2-, and 3-MeV H^+ impact. The agreement of these values with the results of the fit (Table II) is good and confirms that F_{casc} is introduced reasonably.

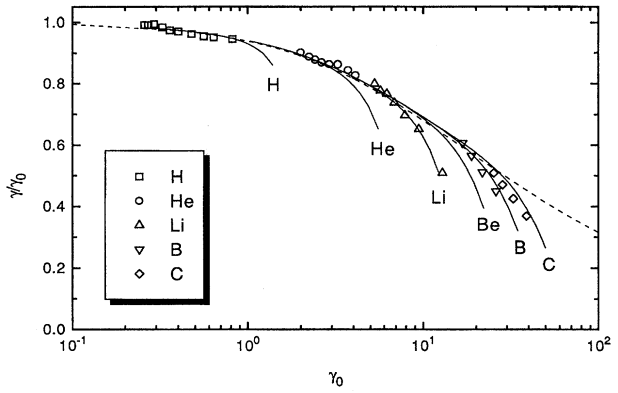

FIG. 3. Emission yields γ normalized to theoretical uncorrected yields γ_0 [Eq. (13)] vs γ_0 for impact of H^+, He^{2+}, Li^{3+}, B^{5+}, and C^{6+} ions on Al. Symbols: experimental yields; full line: fitted theoretical yields [Eq. (14)]; dashed line: theoretical yield in the high-energy approximation [Eq. (17)].

Furthermore, the result of the fit for the Λ parameter can be compared directly with Λ values for H^+ impact [the uncorrected model Eq. (1)]: these values (0.112 for Al, 0.090 for Cu, and 0.101 for Au [9]) are close to but smaller than the fit results, since the positive ion channel is not taken into account.

The fit results for Pd_s cannot be compared directly to values obtained from other measurements. P, the escape probability for electrons excited in the mean escape depth d_s, should be somewhat smaller than 0.5 [3]. This leads to a mean escape depth of about 10 Å, which is almost independent of the target material and appears to be a reasonable value.

Experimental yield values and comparison with results of the modified Borovsky-Suszcynsky model (cf. Sec. IV B), using the parameters of Table II, are shown in Figs. 3–5 for impact of fully stripped ions on Al, Cu, and Au targets. The figures show experimental and theoretical yields normalized to γ_0 [cf. Eq. (13)] as a function of γ_0, which, due to the proportionality of γ_0 to the stopping power S, essentially describes γ/S as a function of S. It can be seen that the theoretical predictions agree within 10% with our experiments.

Projectiles with lower Z and low velocity may have the same stopping power as fast projectiles with high Z. Faster

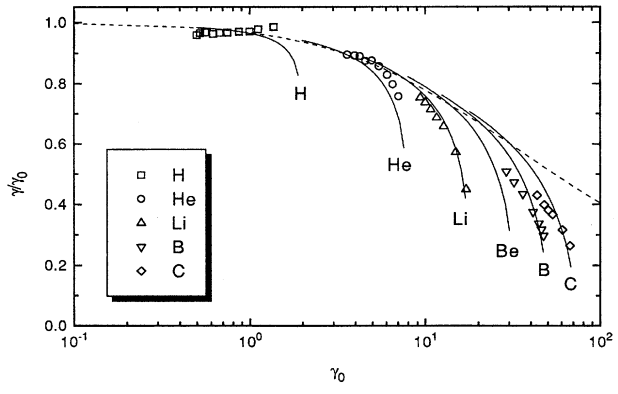

FIG. 4. Same as Fig. 3 for impact on Cu.

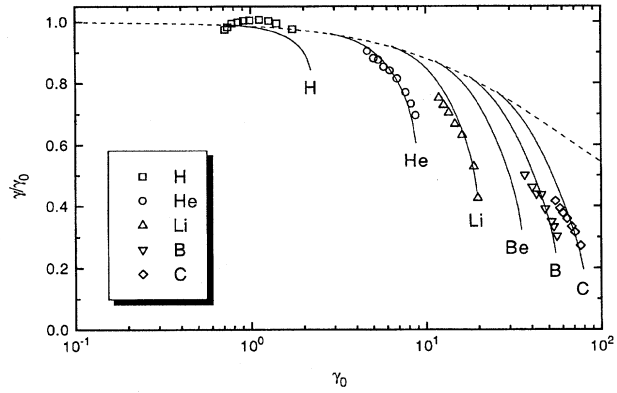

FIG. 5. Same as Fig. 3 for impact on Au.

projectiles will then produce faster primary excited electrons than slower projectiles. Because these faster electrons are less influenced by the positive charge channel than slower electrons, the reduction of the yield is smaller for the faster projectiles than for the slower projectiles, although both have the same stopping power. Therefore, the reduction of the yield depends on both the stopping power, which determines the strength of the positive charge channel, and the projectile velocity, which determines the velocity of the primary excited electrons and therefore the strength of influence of the positive charge channel on the excited primary electrons.

For very high ion velocities the high-energy approximation (Sec. IV C), also shown in Figs. 3–5, is close to the exact numerical results. The corresponding values of the parameter A in Eq. (17) are listed in Table II; they have been calculated using the fit parameters from Table II. As expected, for Al the experimental results are much closer to the high-energy approximation than for the other targets, since for Al the condition $E \gg I$ is fulfilled best. In the remaining discussion we are comparing with the full model only.

There are several possible reasons for the remaining discrepancies between experiment and the theory: (a) the contribution of experimental errors may be 2–3%. (b) Another uncertainty is the charge state of the projectiles within the escape depth of the electrons in the target. Comparing the equilibrium charge states of the projectiles in the target, which are close to Z_{eff} values used in stopping power calculations [16], with the impact charge states, which are equal to the atomic numbers Z, gives that the highest probability for charge changing processes is expected for the C^{6+} ions with lowest velocity. Because charge changing cross sections could not be found for these ions, a rough estimation for this value can be obtained using Eq. (27) in Ref. [8]. The resulting mean distance in a Cu target for electron capture is for 3.2-MeV C^{6+} ions about 2.6 nm, which approximately equals the mean escape depth for electrons. A larger mean distance is expected for Al targets and a smaller one for Au. Therefore electron capture is not expected for H^+, He^{2+}, and Li^{3+} projectiles, but cannot be excluded for B^{5+} and C^{6+} projectiles within the escape depth of the electrons. But the fact that the yields for B^{5+} and C^{6+} impact fit very well the theoretical values confirms the assumption that also for these projectiles charge changing processes can be neglected with respect to the emission of electrons. (c) The deviation of the exact stopping power from the simple scaling law Eq.

(12) can also contribute to the error of the used model. Unfortunately, no experimental investigations are available for the energy range of projectiles used in our work and the contribution of this error can hardly be estimated. From the comparison of the stopping powers S_{th} and S_Z (cf. Sec. III) an error of about 10–20% may be roughly expected.

Furthermore, in Figs. 3–5 it is seen that the agreement between theory and experiment for Al targets is significantly better than for Cu and Au. Here a significant systematic deviation can be observed: projectiles with smaller yields γ_0 (corresponding to high velocities) give smaller experimental yields and projectiles with larger γ_0 (corresponding to low velocities) give larger yields than theoretically expected. Even these deviations are small, and within expected uncertainties of experiment and theory the systematic behavior may indicate a small dependence of Λ[cf. Eq. (1)] on the projectile velocity. A decrease of Λ with increasing projectile velocity is predicted by most theories but has not been observed before [1].

Several other mechanisms have been extensively explored by Borovsky and Suszcynsky [8] that may also give corrections to Eq. (1): they have shown that many mechanisms can be neglected and that the contribution of few cannot be estimated quantitatively. The good agreement of the data presented here with the theoretical predictions based on the positive charge channel corroborates the assumption that this positive charge channel indeed is the dominant effect.

In summary, we present in this paper experimental electron emission yields for bare projectiles. Within the energy range investigated here the following conclusions can be drawn: the ratio of the experimental values to the stopping power of the projectiles in the target layer is (a) not constant, as predicted by basic theories [Sternglass [3], Eq. (1)]. (b) It cannot be expressed as a function of the atomic number alone. (c) It appears to be no function of the stopping power alone. (d) Comparison with theoretical values of the slightly modified model by Borovsky and Suszcynsky [12], however, shows good conformity. This indicates the influence of collective electric fields in the target created by the projectiles on the emission process of the excited electrons.

ACKNOWLEDGMENTS

This work was supported by the Austrian "Fonds zur Förderung der wissenschaftlichen Forschung" Projects No. P07521-PHY and P09504-PHY.

[1] D. Hasselkamp, in *Particle Induced Electron Emission II*, Springer Tracts in Modern Physics Vol. 123 (Springer, Berlin, 1992).
[2] H. Rothard, K. O. Groeneveld, and J. Kemmler, in *Particle Induced Electron Emission II* (Ref. [1]).
[3] E. J. Sternglass, Phys. Rev. **108**, 1 (1957).
[4] J. Schou, Scanning Microsc. **2**, 607 (1988).
[5] H. Rothard, K. Kroneberger, A. Clouvas, E. Veje, P. Lorenzen, N. Keller, J. Kemmler, W. Meckbach, and K. O. Groeneveld, Phys. Rev. A **41**, 2521 (1990).
[6] J. C. Dehaes and A. Dubus, Nucl. Instrum. Methods Phys. Res., Sect. B **78**, 255 (1993).
[7] A. Clouvas, A. Katsanos, B. Farizon-Mazuy, M. Farizon, G. J. Gaillard, and S. Ouaskit, Phys. Rev. B **48**, 6832 (1993).
[8] J. Borovsky and D. Suszcynsky, Phys. Rev. A **43**, 1416 (1991).
[9] O. Benka, E. Steinbauer, and P. Bauer, Nucl. Instrum. Methods Phys. Res., Sect. B **90**, 64 (1994).
[10] A. Koyama, T. Shikata, H. Sakairi, and E. Yagi, Jpn. J. Appl. Phys. **21**, 1216 (1982).
[11] H. Rothard, J. Schou, and K. O. Groeneveld, Phys. Rev. A **45**, 1701 (1992).
[12] J. Borovsky and D. Suszcynsky, Phys. Rev. A **43**, 1433 (1991).
[13] O. Benka, E. Steinbauer, O. Bolik, and T. Fink, Nucl. Instrum. Methods Phys. Res., Sect. B **93**, 156 (1994).
[14] H. Ogawa, I. Katayama, I. Sugai, Y. Haruyama, M. Tosaki, A. Aoki, K. Yoshida, and H. Ikegami, Phys. Lett. A **167**, 487 (1992).
[15] N. Cowern, P. Read, C. Sofield, L. Bridwell, and M. Lucas, Phys. Rev. A **30**, 1682 (1984).
[16] J. F. Ziegler, J. P. Biersack, and U. Littmark, in *The Stopping and Ranges of Ions in Solids* (Pergamon, New York, 1985).
[17] W. Brandt, Nucl. Instrum. Methods **194**, 13 (1982).
[18] J. U. Andersen, G. Ball, J. Davies, W. Davies, J. Forster, J. Geiger, H. Geissl, and V. Ryabov, Nucl. Instrum. Methods B **90**, 104 (1994).
[19] J. D. Jackson and R. L. McCarthy, Phys. Rev. B **6**, 4131 (1972).
[20] O. Benka, A. Schinner, and T. Fink, Phys. Rev. A **51**, 2281 (1995).
[21] S. P. Ahlen, Rev. Mod. Phys. **52**, 121 (1980).